Splitting of Long-Wavelength Modes of the Fractional Quantum Hall Liquid at $\nu = 1/3$

C. F. Hirjibehedin,[1,2,*] Irene Dujovne,[3,2] A. Pinczuk,[1,2,3] B. S. Dennis,[2] L. N. Pfeiffer,[2] and K. W. West[2]

[1]*Department of Physics, Columbia University, New York, New York 10027, USA*
[2]*Bell Labs, Lucent Technologies, Murray Hill, New Jersey 07974, USA*
[3]*Department of Applied Physics and Applied Mathematics, Columbia University, New York, New York 10027, USA*

(Received 17 February 2004; published 2 August 2005)

Resonant inelastic light scattering experiments at $\nu = 1/3$ reveal a novel splitting of the long-wavelength modes in the low energy spectrum of quasiparticle excitations in the charge degree of freedom. We find a single peak at small wave vectors that splits into two distinct modes at larger wave vectors. The evidence of well-defined dispersive behavior at small wave vectors indicates a coherence of the quantum fluid in the micron length scale. We evaluate interpretations of long-wavelength modes of the electron liquid.

DOI: 10.1103/PhysRevLett.95.066803 PACS numbers: 73.20.Mf, 73.43.Lp

The key properties of the two-dimensional (2D) electron liquid phases in the fractional quantum Hall (FQH) regime are embodied in the lowest energy neutral excitations in the quasiparticle charge degree of freedom. These dispersive collective excitations $\Delta(q)$ are built as a superposition of quasiparticle-quasihole dipole pairs separated by a distance $x = ql_0^2$ [1–5], where q is the wave vector and $l_0 = (\hbar c/eB)^{1/2}$ is the magnetic length for a perpendicular magnetic field B. Although the existence of dispersive modes in FQH systems is assumed in theories that represent FQH states as quantum fluids, the modes have been accessible experimentally only at special points in the dispersion. At the best understood FQH state at Landau level filling factor $\nu = 1/3$, the mode energies have been observed in the long-wavelength limit by inelastic light scattering [6–8], at the magnetoroton minimum at $ql_0 \sim 1$ by ballistic phonon studies [9] and light scattering [7,8], and in the large wave vector limit by activated magnetotransport [10–13] and light scattering [8].

The long-wavelength excitations of FQH liquids are of major interest. Such modes manifest the macroscopic length scale of the electron liquid because the existence of a well-defined dispersion, which requires the wave vector to be a good quantum number, is directly related to the extent to which the system can be considered translationally invariant. Studies that map the dispersion in the long-wavelength limit would shed light on the interplay between delocalized states that extend over macroscopic lengths and states that are localized, which is of fundamental importance in the understanding of FQH systems.

Probing the long-wavelength dispersion may also clarify an unresolved issue in the excitation spectrum charge excitations at $\nu = 1/3$. It has been postulated that the lowest energy excitation at long wavelengths could result from a quadrupolelike excitation built from two quasiparticle-quasihole pairs, called a two-roton bound state [5,14,15]. Recent evaluations [16,17] have explored the low-lying charge excitations at $q \to 0$ by computing the energy of a pair of bound rotons with opposite wave vector and found its energy to be below that of the $q \to 0$ mode constructed from single quasiparticle-quasihole pairs. Because a quadrupolelike excitation is predicted to have a qualitatively different dispersion, experimental determinations of the long-wavelength dispersion provide a key probe of the character of the excitations.

We report here the first observation of dispersion in the long-wavelength modes of FQH liquids. By varying the wave vector k transferred to the 2D system in resonant inelastic light scattering experiments, we are able, for the first time, to probe the dispersive behavior of the lower energy charge excitations at $\nu = 1/3$ in the wave vector range $kl_0 \lesssim 0.15$. In the spectra, we find a mode at the lowest k that splits into two distinct modes at $kl_0 \sim 0.1$. The appearance of two distinct branches in the mode dispersion reveals the complex nature of the excitation spectrum at small wave vectors, and is the first direct evidence of the existence of two different FQH excitations at long wavelengths.

The evidence of dispersive long-wavelength excitations provides a unique measure of the macroscopic length scale of the quantum liquid. From the changes in the modes for small changes in the wave vector, we are able to infer that coherence in the quantum fluid occurs in large lakes with macroscopic characteristic lengths that are in the range of $100l_0$ and are in the micron length scale. It is remarkable that behaviors linked to translational invariance occur on this large length scale given that residual disorder must exist in the FQH state.

The observed weak dispersion at long wavelengths offers unique experimental insights into the properties of the FQH liquid and is consistent with predictions [3–5,15,17,18]. Our results indicate that the long-wavelength modes tend to converge as $k \to 0$, suggesting the modes may have some mixed character at small wave vectors [14]. At the largest wave vectors, the higher energy excitation is damped, possibly because of interactions with a two-roton continuum [15,17].

We present results from two 2D electron systems formed in asymmetrically doped GaAs single quantum wells. The 2D electron system in sample A (B) is formed in a $w =$ 250 (330) Å wide well and has a density of 9.1 (5.5) $\times$ 10^{10} cm^{-2} with a mobility of 3.6 (7.2) $\times$ 10^6 cm^2/Vs at 3.8 (0.33) K. Finite well widths weaken interactions in the 2D system. In the simplest approximation, this is related to the ratio w/l_0. For samples A and B at $\nu = 1/3$, these ratios differ by approximately 3%. Samples are mounted on the cold finger of a dilution refrigerator with a base temperature of 45 mK, which is inserted into the cold bore of a 17 T superconducting magnet. The normal to the sample surface is at an angle θ from the total applied magnetic field B_T, making $B = B_T \cos\theta$.

Light scattering measurements are performed through windows for direct optical access, with the laser power density kept below 10^{-4} W/cm^2. The energy of the incident photons ω_L is in resonance with the excitonic optical transitions of the 2D electron system [19,20]. Spectra are obtained in a backscattering geometry, illustrated in the inset of Fig. 1(a). The incident and scattered photons make an angle θ with the normal to the sample surface. The wave vector transferred from the photons to the 2D system is $k = k_L - k_S = (2\omega_L/c)\sin\theta$, where $k_{L(S)}$ is the in-plane component of the wave vector of the incident (scattered) photon. This allows tuning of the wave vector transferred to the 2D system by varying the angle of the sample. For a given θ the value of B_T is tuned such that B corresponds to $\nu = 1/3$. Sufficient signal can be detected for $\theta < 65°$ so that $k \lesssim 1.5 \times 10^5$ cm^{-1}. In our samples at $\nu = 1/3$, this corresponds to $kl_0 \lesssim 0.15$. The uncertainty in the wave vector of the excitations is primarily set by the finite solid angle of collection ($\pm 7°$ from the vertical) and is less than $\pm 0.01/l_0$. We therefore present results from spectra spaced by $\sim 0.02/l_0$ up to the largest accessible k.

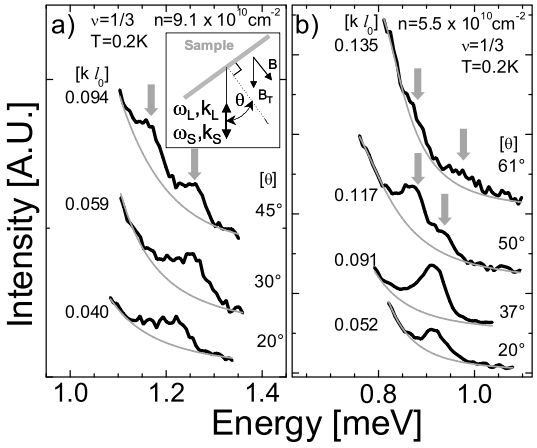

FIG. 1. Inelastic light scattering spectra of low-lying long-wavelength charge modes at $\nu = 1/3$ at various angles θ in (a) sample A and (b) sample B. The spectra are also labeled by the equivalent wave vector $k = (2\omega_L/c)\sin\theta$ in units of $1/l_0$. The gray arrows highlight the splitting of the single peak at small wave vectors into two peaks at larger wave vectors. The light gray lines show the background. The upper inset in panel (a) shows the inelastic light scattering geometry.

Figure 1(a) shows light scattering spectra from the long-wavelength charge density excitation at $\nu = 1/3$ for various values of θ in sample A. The marked angular dependencies reveal that the wave vector of these excitations is equal to the wave vector transferred by the photons to the 2D system ($q = k$). We see that the peak in the spectrum shifts to higher energy for small changes in wave vector. At the largest wave vector accessible at $1/3$ in this system, a remarkable splitting is observed. The two distinct modes are sharp (FWHM < 0.1 meV) and are well separated by 0.1 meV. Similar behavior is also observed in sample B, although, as seen in Fig. 1(b), the energy scale and the shift in the position of the peak are smaller. Because smaller values of B are required to access $\nu = 1/3$ in sample B, we are able to probe the excitations at substantially larger kl_0. At the largest wave vector $kl_0 = 0.135$, we see that the modes are considerably weaker and broader.

The spectra in Fig. 1 offer the first direct evidence for the existence of two distinct FQH modes in the long-wavelength limit at $\nu = 1/3$. A similar k-dependent splitting into two branches is not seen in other excitations. For example, the long-wavelength spin wave [8] remains unchanged throughout the accessible wave vector range reported here.

The dispersion of the FQH excitations provides a measure for the length scale of the coherence in the quantum fluid. For the measurement of a well-defined wave vector dispersion the change in light scattering wave vector δk has to be larger than the wave vector spacing between modes $2\pi/L$, where L is a characteristic length in the fluid. The angular dependence reveals changes in the modes for $\delta k l_0 \sim 0.02$. We may define the lower bound on the macroscopic extent of the incompressible quantum fluid as $L \gtrsim 2\pi/\delta k \sim 2$ μm. It is interesting to note that

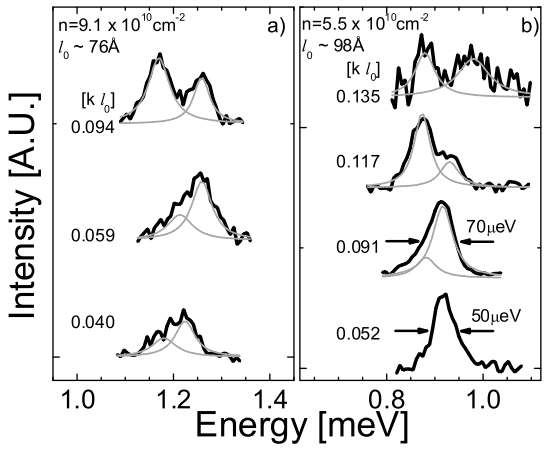

FIG. 2. Spectra from Figs. 1(a) and 1(b) with backgrounds subtracted. The gray lines show fits with two Lorentzian line shapes.

the quantum fluid manifests the properties of translational invariance on these large length scales even in the presence of the residual disorder that must be present in all FQH systems.

In Fig. 2 we show the spectra from Fig. 1 with the backgrounds subtracted. Because two peaks emerge at larger wave vectors, we interpret the single broadened peaks at smaller k as unresolved doublets. These modes show similar dispersive behavior in both samples. To determine the mode energies, we fit all broadened peaks with two Lorentzian modes and label the lower (higher) energy mode $\Delta^{-(+)}(k)$. For the sharpest peak, we use the center of the peak with the uncertainty in the underlying modes estimated by the peak width.

The difference in energy between the peaks is shown in Fig. 3(a) as a function of kl_0. In both samples the modes move farther apart at larger wave vectors. This separation is more pronounced at smaller kl_0 in sample A. We interpret these two modes as two distinct branches of the long-wavelength charge density excitation for the FQH liquid: (i) the long-wavelength limit of the $\Delta(q)$ gap excitation [3–5,18] and (ii) a two-roton state at long wavelengths [5,14–17]. In the long-wavelength limit the $\Delta(q)$ mode is predicted to have a slight downward dispersion, while the two-roton mode is expected to have an upward dispersion. This is in qualitative agreement with our observation that the separation between the modes increases with kl_0, though our results do not allow us to definitively resolve the dispersions of the individual modes.

It is intriguing that the two long-wavelength modes seem to converge as $k \to 0$. Although $\Delta(q)$ is thought to have a purely dipolar character near the roton wave vector q_R, calculations suggest that a purely dipolar mode would have significantly larger energy than a quadrupolar two-roton mode at $k \to 0$ [16,17]. This may indicate that the $\Delta(q)$ mode has a mixed character at small wave vectors, becoming purely dipolar only at larger wave vectors near the roton wave vector q_R [14].

In Fig. 3(b) we show the energy vs kl_0 relations for each individual mode as obtained from the fits, with the energy in units of $e^2/\epsilon l_0$ and the wave vector as kl_0. We have scaled down the energies from the higher density sample A by an additional 4% to account for the difference in finite width effects, so that the mode energies are consistent as $k \to 0$. Included in Fig. 3(b) are possible dispersions for the two modes that are qualitatively consistent with our results. The actual dispersion will be much more complex because it should include interactions between the quasiparticles and the interactions with the continuum of states that is at slightly higher energies [15].

One measure of the two-roton binding energy can be obtained from a comparison of $\Delta(k) \to 0$ and the roton energy $\Delta(q_R)$. In Fig. 4 we show a light scattering spectrum with excitations from critical points in the dispersions at

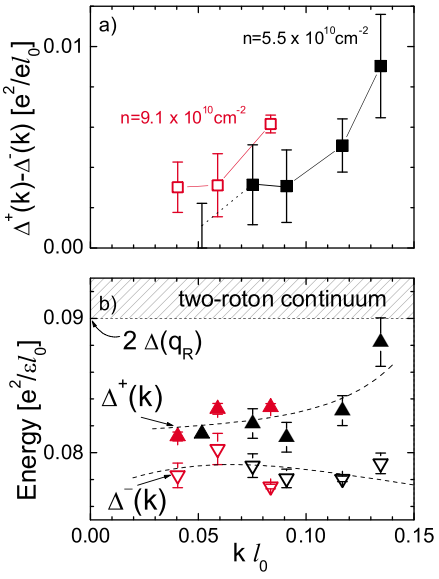

FIG. 3 (color online). (a) Energy difference between the two modes from samples A (red or gray) and B (black) as a function of kl_0 based on fits of spectra. The black bar at $kl_0 = 0.052$ represents the uncertainty in the mode separation based on the linewidth of the observed single peak. (b) Energy vs kl_0 for each individual mode. Open and solid triangles represent energies obtained by fits with two modes from samples A (red or gray) and B (black). Error bars do not include the uncertainty in determining the zero offset ($\lesssim 5 \times 10^{-4} e^2/\epsilon l_0$) for each spectrum. The dashed lines are guides for the eye for possible dispersions of the two modes.

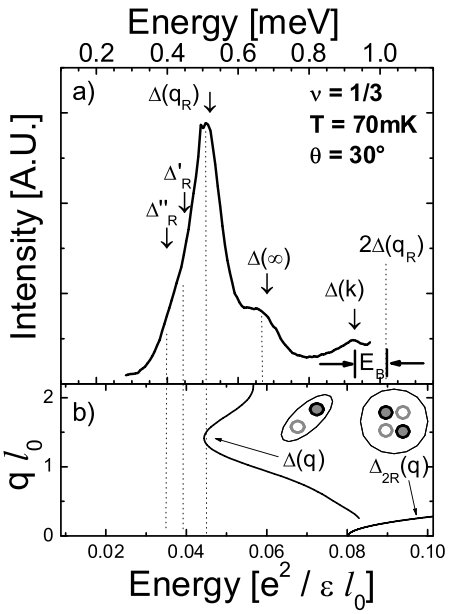

FIG. 4. (a) Spectrum at $\nu = 1/3$ with $\theta = 30°$. The arrows label assigned modes. A number of modes $\Delta(q_R)$, Δ'_R, and Δ''_R are seen in the range of the roton energy. Also indicated is the position of $2\Delta(q_R)$ and E_B. (b) Schematics for the quadrupole-like $\Delta_{2R}(q)$ dispersion [15,17] and the $\Delta(q)$ excitation [3,4,18], which becomes dipolelike at q_R.

$\nu = 1/3$. We find that $\Delta(k)$ is somewhat smaller than $2\Delta(q_R)$. The difference could represent a binding energy $E_B = 0.1$ meV that is 10% of the total two-roton energy. As seen in Fig. 3, the $\Delta^+(k)$ mode approaches the continuum of two-roton states at the largest k. Interactions between $\Delta^+(k)$ and the continuum may be responsible for the dramatic damping effects seen at the largest k and for the differences in the mode separations as a function of kl_0.

In Fig. 4 additional excitations are seen at energies slightly below the roton energy $\Delta(q_R)$. It is surprising to find a number of excitations near the roton because only a single critical point is predicted in the mode dispersion in that energy range [3–5,15,16,21]. These lower energy roton excitations Δ'_R and Δ''_R do not yield a two-roton binding energy when compared to $\Delta(k) \rightarrow 0$. This suggests that although Δ'_R and Δ''_R may be related to roton excitations they would not contribute to the formation of a two-roton bound state. It may be possible for a more complex excitation to be built from a roton and an additional charged object, such as an additional quasiparticle or quasihole [22]. Within such an interpretation, the highest energy roton mode $\Delta(q_R)$ would be the neutral roton excitation, and the lower energy modes Δ'_R and Δ''_R would be charged roton excitations. The difference in energy between the $\Delta(q_R)$ and Δ'_R modes is ~ 0.1 meV. It is unlikely that these modes are rotons bound to impurities because they exists at temperatures well above the 1 K energy difference (not shown).

Activated magnetotransport gaps [10,11], which are found to be lower in energy than the $\Delta(\infty)$ modes with which they are normally associated [13,23], overlap with the energy of the roton modes. The neutral roton is normally not expected to contribute to charge transport [23], though the possibility has been considered [24]. However, a charged roton excitation may be able to participate in such processes. This suggests a possible new role for roton excitations in magnetotransport in FQH states.

In summary, we present the first experimental evidence of two long-wavelength charge density excitations at $\nu = 1/3$ for $kl_0 \lesssim 0.15$. The existence of a dispersion at long wavelengths implies that the FQH liquid is coherent on length scales in the micron range. The two observed branches of the long-wavelength excitation spectrum could be associated with the long-wavelength gap excitation $\Delta(q)$ at $\nu = 1/3$ that may have a dipole-quadrupole character mixed with a two-roton excitation.

We wish to thank J. K. Jain, S. H. Simon, and H. L. Stormer for helpful discussions. This work is supported by the National Science Foundation under Grant No. NMR-03-52738, by the Department of Energy under Grant No. DE-AIO2-04ER46133, and by a research grant from the W. M. Keck Foundation.

*Present address: IBM Research Division, Almaden Research Center, San Jose, CA 95120, USA.

[1] I. V. Lerner and Y. E. Lozovik, Sov. Phys. JETP **55**, 691 (1982).
[2] C. Kallin and B. I. Halperin, Phys. Rev. B **30**, 5655 (1984).
[3] F. D. M. Haldane and E. H. Rezayi, Phys. Rev. Lett. **54**, 237 (1985).
[4] S. M. Girvin, A. H. MacDonald, and P. M. Platzman, Phys. Rev. Lett. **54**, 581 (1985).
[5] S. M. Girvin, A. H. MacDonald, and P. M. Platzman, Phys. Rev. B **33**, 2481 (1986).
[6] A. Pinczuk, B. S. Dennis, L. N. Pfeiffer, and K. West, Phys. Rev. Lett. **70**, 3983 (1993).
[7] H. D. M. Davies, J. C. Harris, J. F. Ryan, and A. J. Turberfield, Phys. Rev. Lett. **78**, 4095 (1997).
[8] M. Kang, A. Pinczuk, B. S. Dennis, L. N. Pfeiffer, and K. W. West, Phys. Rev. Lett. **86**, 2637 (2001).
[9] U. Zeitler, A. M. Devitt, J. E. Digby, C. J. Mellor, A. J. Kent, K. A. Benedict, and T. Cheng, Phys. Rev. Lett. **82**, 5333 (1999).
[10] R. L. Willett, H. L. Stormer, D. C. Tsui, A. C. Gossard, and J. H. English, Phys. Rev. B **37**, R8476 (1988).
[11] R. R. Du, H. L. Stormer, D. C. Tsui, L. N. Pfeiffer, and K. W. West, Phys. Rev. Lett. **70**, 2944 (1993).
[12] K. Park, N. Meskini, and J. K. Jain, Phys. Rev. Lett. **83**, 1486 (1999).
[13] R. H. Morf, N. d'Ambrumenil, and S. Das Sarma, Phys. Rev. B **66**, 075408 (2002).
[14] D.-H. Lee and S.-C. Zhang, Phys. Rev. Lett. **66**, 1220 (1991).
[15] S. He and P. M. Platzman, Surf. Sci. **361**, 87 (1996).
[16] K. Park and J. K. Jain, Phys. Rev. Lett. **84**, 5576 (2000).
[17] T. K. Ghosh and G. Baskaran, Phys. Rev. Lett. **87**, 186803 (2001).
[18] V. W. Scarola, K. Park, and J. K. Jain, Phys. Rev. B **61**, 13 064 (2000).
[19] G. Yusa, H. Shtrikman, and I. Bar-Joseph, Phys. Rev. Lett. **87**, 216402 (2001).
[20] C. F. Hirjibehedin, I. Dujovne, I. Bar-Joseph, A. Pinczuk, B. S. Dennis, L. N. Pfeiffer, and K. W. West, Solid State Commun. **127**, 799 (2003).
[21] T. Nakajima and H. Aoki, Phys. Rev. Lett. **73**, 3568 (1994).
[22] K. Park, Solid State Commun. **121**, 19 (2001).
[23] F. C. Zhang and S. Das Sarma, Phys. Rev. B **33**, R2903 (1986).
[24] P. M. Platzman, S. M. Girvin, and A. H. MacDonald, Phys. Rev. B **32**, R8458 (1985).